RSC Mechanochemistry

ROYAL SOCIETY OF CHEMISTRY

PAPER

View Article Online
View Journal

Cite this: DOI: 10.1039/d5mr00106d

Shaping coordination polymers by ball milling

Giorgio Cagossi, [a] Beatrice Piombo, [a] Andrea Daolio, [a] Paolo P. Mazzeo, [a] Alessia Bacchi [a] and Paolo Pelagatti *[ab]

Received 22nd August 2025
Accepted 1st December 2025

DOI: 10.1039/d5mr00106d

rsc.li/RSCMechanochem

Selective syntheses of known 1D-coordination polymers derived from the combination of 4,4′-bipyridine (**bipy**) or 1,2-bis-(4-pyridyl)ethylene (**dpe**) with $Zn(OAc)_2 \cdot 2H_2O$ were achieved under mechanochemical conditions by carefully controlling the mechanochemical parameters, including reaction stoichiometry and the nature of the solvent used in liquid assisted grinding. Ligand exchange reactions performed under grinding conditions showed the conversion of the **dpe**-containing polymers into **bipy**-containing polymers, whereas the reverse reactions proved unfeasible. A computational rationale for the observed reactivity is provided. The dimensionality growth of the **dpe**-containing 1D-coordination polymers into a three-dimensional pillared metal–organic framework was achieved by reaction with terephthalic acid. The same 3D-MOF was also obtained by a one-pot procedure, involving dpe, $Zn(OAc)_2 \cdot 2H_2O$ and terephthalic acid simultaneously ground in the presence of a small aliquot of *N*,*N*-dimethylformamide. All the reactions occurred in high yields affording pure products with a favorable environmental profile, as evidenced by the environmental factor (EF) and reaction mass efficiency (RME) calculated for selective reactions. This work highlights how mechanochemistry not only allows the efficient synthesis of coordination polymers but also their post-synthetic modifications by environmentally benign protocols.

Introduction

Mechanochemistry represents a unique way of conducting a chemical reaction based on the grinding of solid reagents.[1–3] This is usually performed using a ball-mill apparatus, where solid particles are ground inside a rigid container by means of accelerated balls.[4] Since it removes the need of a solvent, mechanochemistry is intrinsically green as it produces virtually no waste.[5,6] Moreover, under these conditions, so-called "impossible reactions"[7] – reactions involving highly insoluble reagents – are promoted. Hence, the popularity of mechanochemistry is raised among the synthetic chemists, although there is often low understanding of the nature of the events that govern the reactions under milling conditions.[8–10] Among the porous cutting-edge functional materials, Metal–Organic-Frameworks (MOFs) have a prominent role.[11–13] MOFs are coordination polymers (CPs) derived from the combination of metal-containing secondary-building-units (SBUs) interconnected by organic linkers. Their importance in fields where porosity plays a crucial role is well-known and extensively reviewed.[14–16] Despite the huge number of structurally characterized MOFs, examples of their industrial applications are scarce.[17] One of the main drawbacks that hamper MOF implementation is the low scalability of their synthesis, often based on solvothermal reactions. Although the solvothermal route makes possible the isolation of X-ray quality single crystals, fundamental for the full understanding of their hosting capacity, the use of high boiling and toxic solvents, long reaction times and, often, unsatisfactory yields negatively impact the cost-effectiveness and viability of the final materials. It follows that the mechanochemical synthesis of MOFs is highly attractive as shown by the number of publications appeared in the last few years, with some dedicated reviews.[18–20] Among the different types of MOFs reported in the literature, a pivotal role is played by mixed-ligand MOFs (ML-MOFs).[21,22] Often, ML-MOFs are made by square planes containing SBUs connected by dicarboxylate linkers, then pillared by neutral ones such as bis-pyridines,[23–25] giving rise to porous frameworks labeled pillared-MOFs (PL-MOFs). The presence of two different linkers allows for high degrees of functionalization that translate into highly versatile crystalline materials.[26,27] Although step-wise constructions of PL-MOFs in solution[28,29] and on planar surfaces were successfully performed,[30–32] the single reactive steps that lead to the assembly of the final 3D architecture are poorly understood. The mechanochemical synthesis of PL-MOFs counts a limited number of examples,[33–37] but efforts in this direction are highly desirable. In particular, the stepwise construction of PL-MOFs under mechanochemical conditions is of particular relevance for demonstrating the feasibility of well-controlled and selective processes in non-conventional reactive environments. The number of reports addressing the stepwise mechanochemical construction of PL-MOFs is

[a]Department of Chemical Sciences, Life Science and Environmental Sustainability, University of Parma, Parco Area delle Scienze 17/A, 43124 Parma, Italy. E-mail: paolo.pelagatti@unipr.it

[b]Interuniversity Consortium of Chemical Reactivity and Catalysis (C.I.R.C.C.), Via Celso Ulpiani 27, 70126 Bari, Italy

scarce.[34,38,39] Likewise, the number of papers dealing with mechanochemical post-synthetic modifications (MPSMs) of CPs involving linker exchange is also limited.[40,41] Therefore, efforts in this direction are highly desirable. In our laboratory we have solid experience in the mechanochemical synthesis of different types of materials such as organic co-crystals containing active pharmaceutical ingredients,[42–45] hybrid materials derived from the combination of lignin and inorganic nanocrystals,[46–48] as well as metal complexes[49] and coordination polymers.[50] Contributing to the development and understanding of the mechanochemical preparation of MOFs, we decided to build PL-MOFs through a stepwise, bottom-up approach, whose experimental design is depicted in Fig. 1. It involves a first step dedicated to the assembly of 1D-CPs derived from the reaction of rigid bis-pyridine-containing linkers, in particular 4,4′-bipyridine (**bipy**) and 1,2-bis-(4-pyridyl)ethylene (**dpe**) with $Zn(OAc)_2 \cdot 2H_2O$ (Fig. 1, path a or a′). 1D-CPs are subsequently reacted with terephthalic acid (**H_2ta**) to form the target PL-MOFs (Fig. 1, path b or b′) *via* substitution of the acetate anion with **ta^{2-}** dianions. Finally, a one-pot procedure involving the simultaneous grinding of the three reagents (metal salt, bis-pyridine-linker and **H_2ta**) is also performed (Fig. 1, path c), and the results are compared with those coming from paths a and b. The progress of each reaction was monitored by *ex situ* powder X-ray diffraction analysis (PXRD), comparing the diffractograms of the ground materials with those calculated from the known crystalline structures deposited in the CCDC databank. Moreover, MPSMs were also performed to assess the conversion of one 1D-CP into another by linker exchange, as depicted in Fig. 1 (path d). The two pyridine linkers, bipy and dpe, were chosen based of the following considerations: (i) solution syntheses of 1D-CPs derived from the reaction of the two linkers with $Zn(OAc)_2$ are known; (ii) different crystalline structures are reported, whose formation depends on the adopted experimental conditions (*vide infra*); (iii) the structures differ in framework topology and type of SBUs contained in the polymeric chains.

Similarly, the dicarboxylate linker **ta^{2-}** was chosen on the basis of the following considerations: (i) **H_2ta** is expected to replace the basic AcO^- anions as AcOH, which, owing to its volatility, can easily leave the reaction medium, thus avoiding the use of an external base that would inevitably lead to the formation of a salt byproduct; (ii) ML-MOFs containing **ta^{2-}**, **bipy** or **dpe**, and Zn^{2+} obtained by solution syntheses are known; (iii) their structures present different crystalline frameworks and SBUs (*vide infra*). The adopted mechanochemical approach is particularly attractive since it allows evaluation of the convergence of the different reactive pathways reported in Fig. 1 and, at the same time, to compare the results obtained with solution syntheses. Given the different reactive environments, mechanochemical and wet reactions can lead to different products, an aspect that is of particular interest.

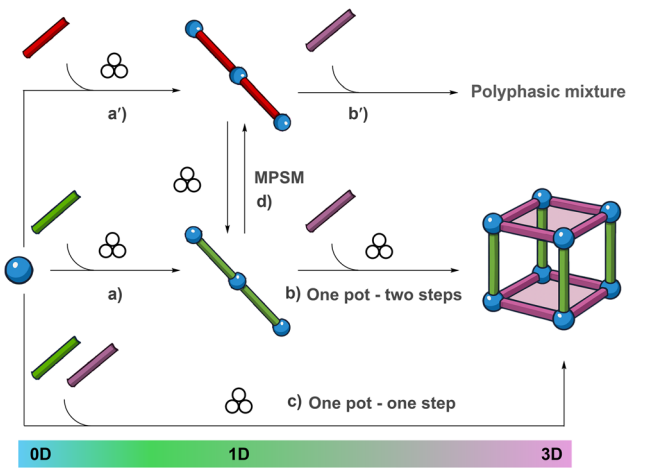

Fig. 1 Schematic representation of the experimental design followed for the construction of the PL-MOF. Path a or a′: from a 0D to a 1D-CP (color code: Zn blue, **bipy** red, and **dpe** green); path b: from a 1D-CP to a PL-MOF (one pot – two steps; color code: **H_2ta** purple); path c: from a 0D to a PL-MOF (one pot – one step); path d: mechanochemical post-synthetic modification of 1D-CPs (linker exchange).

Results and discussion

Structural background from CPs synthesized in solution

The linearity of the two ligands **bipy** and **dpe** is ideal for the construction of CPs of different dimensionality and examples of 1D and 3D polymers can be found in the literature. A structural search on the Cambridge Structural Database (CSD) revealed the presence of two 1D-CPs containing bipy, Zn^{2+} and acetate anions. In one case, here referred to as CP1-**bipy**, the polymer has a ladder structure with a SBU of formula $[Zn_2(\mu\text{-}OAc)_2(\kappa^2\text{-}OAc)_2(py)_4]$ (Fig. 2, CSD Refcode: ALUPUS), wherein each Zn^{2+} ion is octahedrally surrounded by two oxygen atoms belonging to two bridging acetate anions, two oxygens of a κ^2-chelating acetate anion and two pyridine rings. The formula of the polymer is $[Zn_2(OAc)_4(bipy)_2]_n$. The polymer was synthesized either under hydrothermal conditions[51] or at room temperature in organic solvents[52] (ethanol/dichloromethane mixture) with a **bipy** : Zn molar ratio of 1 : 1. A different framework, composed by zig–zag chains of formula $[Zn_2(OAc)_4(\mathbf{bipy})]_n$, here referred to as **CP0-bipy** (Fig. 2, CSD Refcode: EYELID), was obtained at room temperature in methanol when an excess of metal was used.[53] The SBU is less symmetrical that the one found in **CP1-bipy**, its formula being $[Zn_2(\mu\text{-}OAc)_2(\kappa^2\text{-}OAc)(\kappa^2/\mu\text{-}OAc)(py)_2]$. The two metals display different coordination environments, octahedral and trigonal bipyramidal. In the CSD, there are three structurally known 1D-CPs containing **dpe**, Zn^{2+} and acetate anions. One structure, here referred to as **CP2-dpe** (Fig. 2, CSD Refcode: MANMEU), contains the same SBU found in **CP1-bipy**, with which it is isoreticular, its formula being $[Zn_2(OAc)_4(\mu\text{-}\mathbf{dpe})_2]_n$.[54] It was obtained by buffering a MeOH solution of the salt and a THF solution of the linker with ACN, using a 1 : 1 **dpe** : salt molar ratio. The same polymer was also obtained by slow evaporation of a methanol solution containing equimolar amounts of the reagents. The same reaction conducted in DMF and then in hot water led instead to a 1D-CP where **dpe** bridges tetrahedrally coordinated Zn^{2+} ions (**CP3-dpe**, Fig. 2, CSD Refcode: BUJDES), containing infinite 1D zig–zag chains with SBUs of the type $[Zn(OAc)_2(py)_2]$. Each metal coordinates two κ^1-

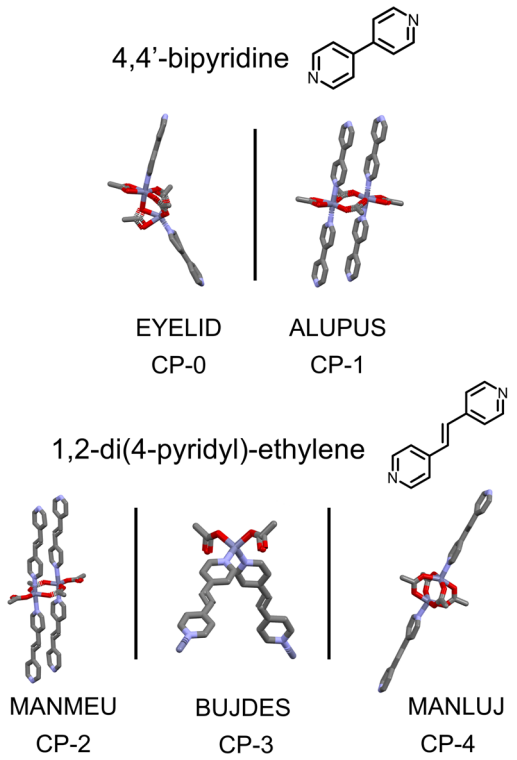

Fig. 2 Structures of the 1D-CPs obtained from $Zn(OAc)_2$ and **bipy** (top) or **dpe** (bottom). The naming refers to the CCDC ref. codes of the corresponding crystalline structures. Color code: Zn purple, N blue, O red, and C grey. Hydrogen atoms are omitted for clarity.

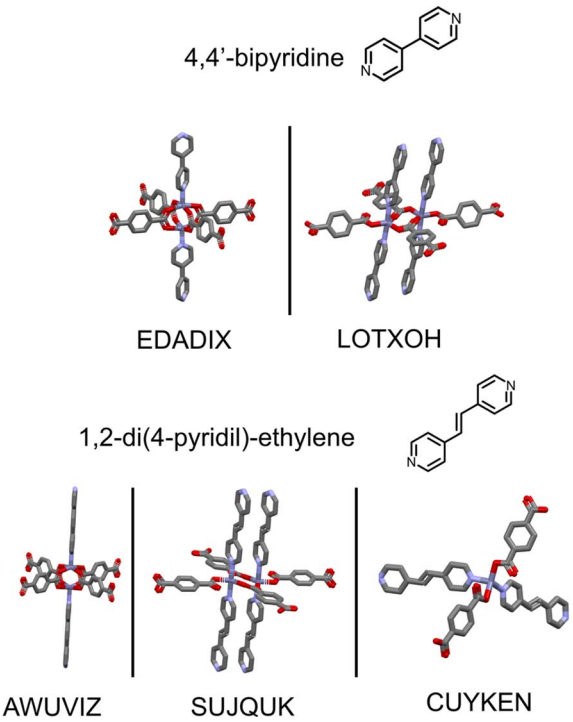

Fig. 3 Structures of the ML-MOFs obtained from Zn^{2+}, $\mathbf{ta}^{2-}$ and **bipy** (top) or **dpe** (bottom). Under each structure is reported the CSD Refcode of the corresponding crystalline structures. Color code: Zn purple, N blue, O red, and C grey. Hydrogen atoms are omitted for clarity.

monodentate acetate anions, for a whole polymer formula corresponding to $[Zn(OAc)_2(\mu\text{-}\mathbf{dpe})]_n$. The same framework was also isolated from a reaction between $Zn(NO_3)_2\cdot 6H_2O$, **dpe** and NaOAc in a H_2O/EtOH mixture at room temperature.[55] Finally, a polymer of formula $[Zn_2(OAc)_4(\mu\text{-}\mathbf{dpe})]_n$ was obtained when a methanol solution of $Zn(OAc)_2\cdot 2H_2O$ and a THF solution of the ligand were buffered by a methanol layer.[54] In this case, linear 1D chains containing paddle-wheel SBUs of formula $[Zn_2(OAc)_4(py)_2]$ bridged by **dpe** were found (**CP4-dpe**, Fig. 2, CSD Refcode: MANLUJ). The SBUs contained in the frameworks of the PL-MOFs derived from the combination of $\mathbf{ta}^{2-}$, Zn^{2+} and **bipy**/**dpe** are shown in Fig. 3. Two different structures containing **bipy** are known (Fig. 3, left). One case corresponds to a two-fold interpenetrated cubic lattice composed by squares containing paddle-wheel SBUs bridged by dicarboxylate anions and pillared by **bipy** linkers (CSD Refcode: EDADIX).[56]

The formula of the SBU is $[Zn_2(COO)_4(py)_2]$, while the formula of the framework is $[Zn_2(\mathbf{ta})_2(\mathbf{bipy})]_n$. The crystals grew under solvothermal conditions, in a DMF/EtOH mixture, using $Zn(NO_3)_2\cdot 6H_2O$ as the salt. A second two-fold interpenetrated prismatic framework was obtained by conducting the solvothermal reaction in pyridine (CSD Refcode: LOTXOH).[57] In this case, the SBU has the formula $[Zn_2(\mu\text{-}COO)_2(\kappa^1\text{-}COO)_2(py)_2]$, where each Zn ion has trigonal bipyramidal coordination, satisfied by two oxygens of two bridging carboxylates, one oxygen of a κ^1-monodentate carboxylate and two pyridine rings. In this case, the formula of the framework is $[Zn_2(\mathbf{ta})_2(\mathbf{bipy})_2]_n$.

Three ML-MOFs containing **dpe**, $\mathbf{ta}^{2-}$ and Zn^{2+} have been reported in the CSD (Fig. 3, right). In one case (CSD Refcode: AWUVIZ), the not-interpenetrated cubic net has the typical pillared structure, with paddle-wheel SBUs of the type $[Zn_2(COO)_4(py)_2]$ and a framework formula corresponding to $[Zn_2(\mathbf{ta})_2(\mathbf{dpe})]_n$. It was isolated from an unexpected thermal decomposition of a bis-phenyl tetracarboxylic ligand in DMF at 105 °C.[58] A different framework was isolated through an elaborate layered crystallization, where **dpe** (MeOH) and $Zn(NO_3)_2\cdot 6H_2O$ (water) reacted with a mixture of $\mathbf{H_2ta}$ and triethylamine (EtOH) in the presence of a buffer of MeOH and DMF. In this case, a doubly interpenetrated PL-MOF was isolated, whose framework has the formula $[Zn_2(\mathbf{ta})_2(\mathbf{dpe})_2]_n$. Here, planes containing SBUs similar to those found in **CP2-dpe** are pillared by **dpe** linkers (CSD Refcode: SUJQUK in Fig. 3, right).[59] Finally, a third structure was obtained reacting equimolar amounts of $Zn(NO_3)_2\cdot 6H_2O$, **dpe** and $\mathbf{H_2ta}$ under hydrothermal conditions.[60] Here, tetrahedral SBUs where Zn^{2+} is surrounded by two pyridines and two κ^1-monodentate acetates are contained in a diamondoid net (CSD Refcode: CUYKEN in Fig. 3, right), for a whole framework formula $[Zn(\mathbf{ta})(\mathbf{dpe})]_n$.

Background of mechanochemically synthesized CPs containing bipy and dpe

The number of 1D-CPs mechanochemically synthesized containing **bipy** is very limited compared with those derived from solution syntheses. To the best of our knowledge, there is only

one report dealing with the mechanochemical reaction involving **bipy** and $Zn(OAc)_2$.[61] The reaction was conducted by manually grinding equimolar amounts of the two reagents, and led to **CP1-bipy**. A sonochemical synthesis of the same polymer conducted in ethanol has also been published.[62] A slightly higher number of reports can be found regarding other transition metal salts, such as MX_2 (M = Co, Zn, Pt; X = Cl or Br).[63–65] Finally, a series of nitrate-containing polymers with different transition metals have been prepared by ball-milling and twin-screw extrusion.[66] In most cases, the PXRD traces were indicative of the formation of the same products isolated in solution. Similarly, there are only two reports dealing with the mechanochemical synthesis of 1D-CPs containing **dpe**. In one case, the linker bridges heteronuclear Fe_3SCu_2 clusters in 2D-assemblies,[67] obtained by grinding the dianion $[Fe_3S]_2^-$ with $[Cu(ACN)_4]^+$ and **dpe** under Liquid Assisted Grinding (LAG) conditions. The other CP derives instead from the grinding of a diphosphonic acid, **dpe** and $Cu(OAc)_2$ under LAG conditions.[68] In both cases, the structures were confirmed by PXRD analysis by comparison with the known single-crystal deposited data.

A rather limited number of examples dealing with the mechanochemical synthesis of ML-MOFs containing **bipy** can be found. In combination with $\mathbf{H_2ta}$ and ZnO under LAG conditions, the two-fold interpenetrated PL-MOF $[Zn(\mathbf{ta})(\mathbf{bipy})]_n$ (CSD Refcode: LOTXOH) was isolated (Fig. 3, left).[34] Other mechanochemically synthesized pillared MOFs contain fumarate,[34] diphosphonate[37] and bent dicarboxylate linkers.[69] In the only report regarding PL-MOFs containing **dpe**, the product was obtained grinding fumaric acid, ZnO and **dpe** under LAG conditions.[34] Based on PXRD characterization, it was assumed to be a two-fold interpenetrated cubic framework analogous to that found for the structurally characterized homologous Cu-MOF,[70] containing paddle-wheel SBUs.

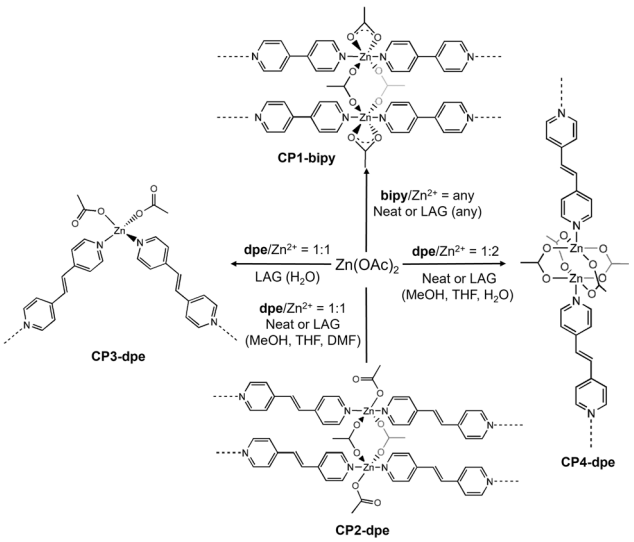

Scheme 1 1D-CPs mechanochemically synthesized and described in this work. The different linker/Zn^{2+} molar ratios and LAG agents are reported for each reaction. The water of crystallization of the metal salt has been omitted. See the Experimental section for details.

Synthesis of the 1D-CPs conducted in this work

The mechanochemical syntheses of the 1D-CPs are depicted in Scheme 1. The experimental conditions adopted for each reaction are provided in Table 1. When equimolar amounts of $Zn(OAc)_2 \cdot 2H_2O$ and **bipy** were ground using an agate mortar and pestle, the quantitative formation of **CP1-bipy** was observed within 60 minutes, as previously reported (Table 1-entry 1 and Scheme 1).[61] To transfer the process to ball milling, we carried out an optimization of the reaction conditions, selecting this synthesis as a model reaction and using MeOH as the LAG agent. *Ex situ* PXRD monitoring at different reaction times revealed the selective formation of the polymer within the first minute of grinding, with 60 minutes required to ensure complete reagent consumption and, importantly, a high degree of crystallinity (Table 1-entry 1 and Fig. 4, orange trace). Fig. S1 collects the PXRD traces acquired at different grinding times. Repeating the same reaction under neat grinding conditions again led to the complete and selective formation of **CP1-bipy**, though with significantly lower crystallinity (Table 1, entry 1 and Fig. S2 for PXRD traces). We further investigated the influence of several milling parameters. Increasing the milling frequency from 20 Hz to 30 Hz did not lead to significant differences in the outcome (Fig. S3). Likewise, the use of milling balls with different diameters (7 mm or 10 mm) had no appreciable effect. Finally, a range of solvents were tested as LAG additives (η = 0.3), such as DCM, ACN, THF, DMF and H_2O, but none of them affected neither the selectivity and yield of the reaction nor the crystallinity of the final product (Table 1-entry 1 and Fig. 4; see Fig. S4 for PXRD traces). In an attempt to direct the synthesis towards **CP0-bipy**, the reaction was repeated using a two-fold excess of the metal precursor and MeOH as the LAG solvent (η = 0.3), consistently with the conditions used in the solution-phase synthesis of **CP0-bipy**.[53] However, after 60 minutes of grinding, PXRD analysis showed the exclusive formation of **CP1-bipy** alongside unreacted $Zn(OAc)_2 \cdot 2H_2O$ (Table 1, entry 1 and

Table 1 Experimental conditions for the synthesis of the 1D-CPs[a]

Entry	Ligand	Ligand/Zn^{2+} molar ratio	LAG additive (h = 0.3)	Product
1	**bipy**	1 : 1, 1 : 2 or 1 : 3	Neat, MeOH, DCM, ACN, THF, DMF	CP1-**bipy** $[Zn_2(OAc)_4(\mu\text{-bipy})_2]_n$
2	**dpe**	1 : 1	Neat, MeOH, THF, DMF	CP2-**dpe** $[Zn_2(OAc)_4(\mu\text{-dpe})_2]_n$
3	**dpe**	1 : 1	H_2O	CP3-**dpe** $[Zn(OAc)_2(\mu\text{-dpe})]_n$
4	**dpe**	1 : 2	Neat, MeOH, THF, H_2O	CP4-**dpe** $[Zn_2(OAc)_4(\mu\text{-dpe})]_n$

[a] Reaction conditions: ball-mill frequency: 20 or 30 Hz; grinding time: 60 minutes; ball ∅ = 7 or 10 mm.

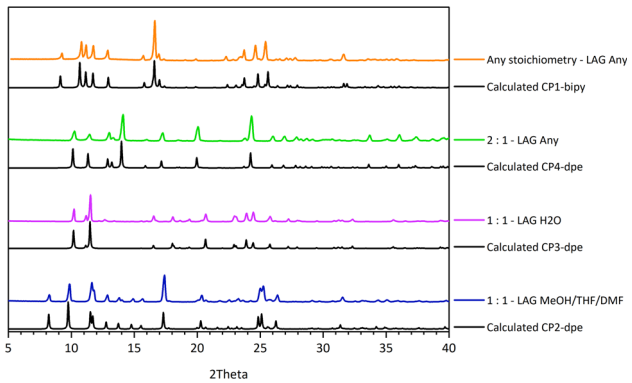

Fig. 4 XRPD traces of the mechanochemical 1D-CPs obtained under different reaction conditions after 60 minutes of grinding. The Zn : dpe molar ratios and LAG agents are reported next to the experimental traces. The traces calculated from the crystalline structures are reported next to the names of the corresponding 1D-CPs. The traces of the products obtained under neat grinding are provided in the SI.

Fig. S5 for PXRD traces). Additional tests using various stoichiometric ratios of **bipy** and $Zn(OAc)_2 \cdot 2H_2O$ similarly resulted in no products other than **CP1-bipy** and the unreacted starting material (Table 1, entry 1). These results suggest that, under mechanochemical conditions, the formation of the ladder motif is strongly favoured. From literature data referring to solution syntheses,[54] it appears that the type of 1D-CP that forms from the reaction between **dpe** and $Zn(OAc)_2$ strongly depends on the solvent used, regardless of the stoichiometry of the reaction. To test if the same solvent effect could be observed under mechanochemical conditions, parallel reactions between equimolar amounts of **dpe** and $Zn(OAc)_2 \cdot 2H_2O$ were conducted using liquid-assisted grinding with the solvents employed in the solution syntheses. In all cases, the parameter η was set to 0.3. In solution, **CP2-dpe** forms in pure MeOH or by a layering of MeOH, THF and ACN. Under grinding, this polymer forms when MeOH, THF or DMF are used as LAG agents (Table 1-entry 2 and Scheme 1), as evidenced by PXRD analysis (Fig. 4). The use of either ACN or DCM was instead unsuccessful, leaving the reagents practically intact. The use of water as the LAG agent led instead to **CP3-dpe** (Table 1-entry 3, Scheme 1 and Fig. 4, purple trace), in line with what is observed in solution.[54,55] It follows that the use of equimolar amounts of reagents leads to the formation of the frameworks featured by the same Zn : **dpe** ratio, where the type of SBU is dictated by the solvent. In no case the formation of the paddle-wheel containing polymer, **CP4-dpe**, was observed. Actually, this polymer corresponds to a Zn : **dpe** ratio of 2 : 1, and in solution it forms by layering MeOH and THF solutions of the reagents.[54] Then, to promote the formation of **CP4-dpe**, the reaction was repeated in either MeOH or THF using a Zn : **dpe** molar ratio of 2 : 1 (Table 1-entry 4 and Scheme 1).

Under these conditions, the formation of **CP4-dpe** was observed, as indicated by PXRD analysis (Fig. 4, green trace). It is worth noting that the use of H_2O as the LAG agent did not affect the reaction, provided the same Zn : **dpe** molar ratio (Table 1-entry 4 and Fig. 4). Notably, in all cases, the complete conversion of the reagents was observed within 60 minutes of grinding. Fig. S6 collects all the PXRD traces obtained with different LAG agents and stoichiometries.

Finally, the neat grinding of equimolar amounts of the reagents led to the formation of **CP2-dpe**, while the same reaction repeated using a Zn : **dpe** molar ratio of 2 : 1 led to **CP4-dpe** (Table 1-entries 2 and 4).

On the base of the synthetic results, the following considerations can be traced back: (1) regardless of the solvent used as the LAG agent, **bipy** leads exclusively to the ladder polymer **CP1-bipy**, even when a two-fold excess of metal, expected to favor the formation of **CP0-bipy**, is applied; (2) **dpe** shows a higher structural variability that can be tuned by a judicious selection of reaction stoichiometry and liquid used as the LAG agent. In particular, the chosen reaction stoichiometry selects the type of CP that forms. When a Zn : **dpe** = 1 : 1 molar ratio is applied, **CP2-dpe** forms irrespective to the solvent used as LAG agent, with the exception of water that leads to **CP3-dpe**. Conversely, when a Zn : **dpe** = 2 : 1 molar ratio is chosen, the paddle-wheel containing **CP4-dpe** forms, irrespective to the liquid used as the LAG agent, water included. The solvent induced selectivity does not seem ascribable to a template effect of the solvent molecules, since all the isolated products were devoid of traces of solvents, as indicated by FTIR spectroscopy (see Fig. S14–S18).

Rationalization of reaction selectivity and formation of 1D-CPs

In silico simulations were conducted to obtain additional insights into the performed reactions (summarized in Fig. 5). A preliminary assessment of the relative stabilities of the possible zinc coordination polymers was performed through the program Gaussian16.[71] The free energy of reaction (schematized in Fig. 5A, above) of minimal SBUs composed of zinc metals and acetate and pyridine (**py**) capping ligands was computed in vacuum and in the three solvents (SMD method) H_2O, MeOH and DMF (Fig. 5A), considering the ligand arrangements derived from the complete substitution of the two molecules of water contained in the starting salt. The SBU contained in **CP0-bipy** is labelled as "D-PW", the SBU contained in **CP1-bipy** and **CP2-dpe** as "Ld", the SBU contained in **CP3-dpe** as "Tet" and, finally, the SBU contained in **CP4-dpe** as "PW". When a Zn : **py** molar ratio of 1 : 1 is considered, corresponding to a Zn : linker ratio of 2 : 1 (linker = **bipy** or **dpe**), the paddlewheel-type SBU is always preferred, with the SBU featuring **CP0-bipy** being much less stable during the optimization process. This is in line with the experimentally observed tendency to produce **CP4-dpe** regardless of the solvent used as the LAG agent. When instead a Zn : py ratio of 1 : 2 is considered, corresponding to a Zn : linker ratio of 1 : 1, the "Ld" complex (corresponding to the isolated **CP1-bipy** or **CP2-dpe**) is often preferred to "Tet" (in line with the experimental analysis) with the exception of water solvation. In this solvent, the "Ld" coordination is disfavored, so that the "Tet" one (corresponding to the isolated **CP3-dpe**) is the most stable. Although the milling experiments were conducted under LAG conditions and not in solution, the calculations strongly suggest that the medium polarization induced by the

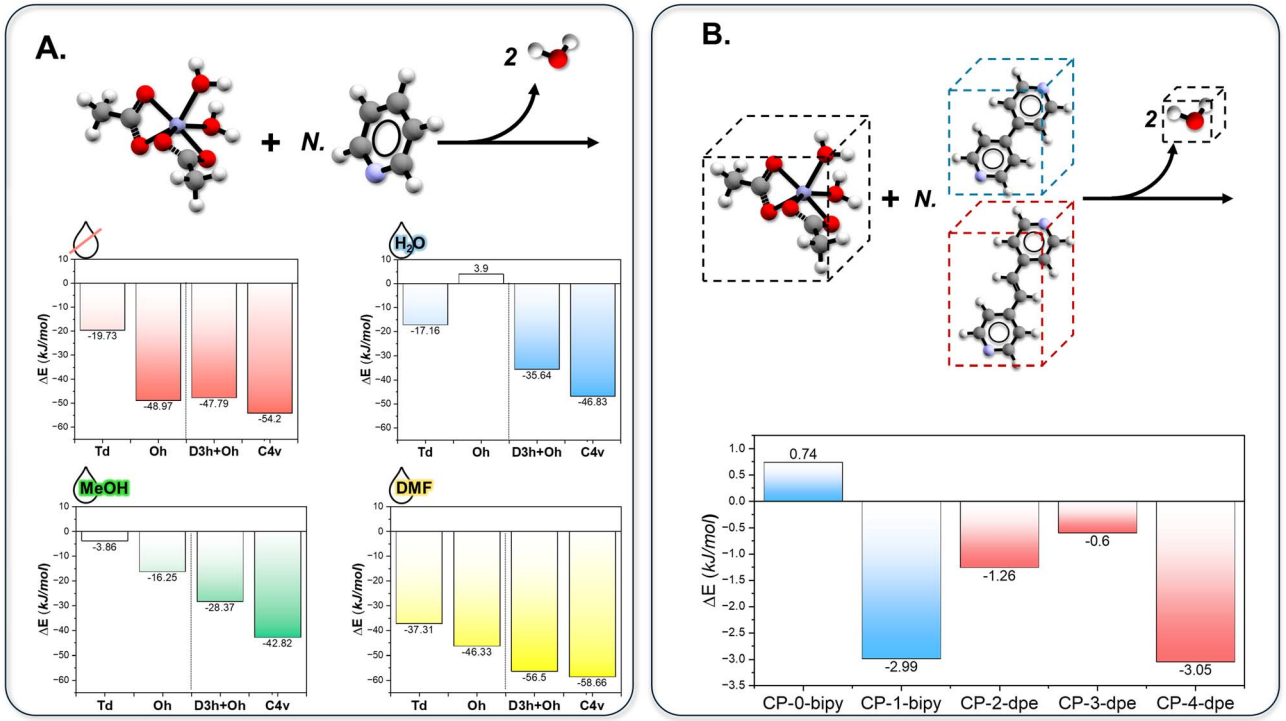

Fig. 5 Summary of the computational simulations performed for this work. (A) Summary of the free energy of reaction for all the simulations performed on non-periodic systems. The model reaction is schematized above, while the free energy of the reaction is collected in different bar plots at the bottom of the panel, grouped by the solvent employed in the SMD method. A dashed line divides the different stoichiometries considered. (B) Summary of the free energy of reaction for all the simulations performed on periodic systems. The reaction of formation of the complexes is schematized above, while the stabilization energies of the reaction is collected in a bar plot at the bottom of the panel; blue bars represent the formation of coordination polymers in which bipy is present, and red bars represent the formation of coordination polymers in which dpe is present. To allow for a useful comparison between complexes with different stoichiometries and structures with different *Z* factors, the energy is provided per mole of Zn.

solvent during the formation of the SBU might be a prime factor in the formation of a specific crystalline phase, also in line with the solution experiments already performed.[54] Considering the coordination environment of Zn in the different SBUs, it turns out that "Tet" is favored when water is involved. Additional information regarding the relative stability of the crystalline phases can be retrieved from periodic simulations by means of the program CASTEP.[72] Simulating the reaction enthalpy of the performed experiments (Fig. 5B), the results show that the formation of **CP0-bipy** is thermodynamically disfavored, while **CP1-bipy** is strongly stabilized. It follows that, in the formation of the two 1D-CPs containing **bipy**, the marked difference in stability of the two possible crystalline phases plays a crucial role, likely sufficient to promote the formation of **CP1-bipy** in any of the solvent analyzed, even in water, where the formation of the SBU by itself is thermodynamically disfavored, or when different stoichiometric ratios are employed.

Post-synthetic modifications of 1D-CPs (MPSMs)

In the attempt to enlarge the number of CPs containing **bipy** mechanochemically synthesized, we directed our attention to the possibility of exchanging **dpe** with **bipy** from CPs of the first, through MPSMs (Scheme 2). Provided that no change of the SBU occurs during grinding, this approach could, in principle, lead to new **bipy**-containing CPs.[73] To test the possibility of a simple linker exchange, we first reacted **CP2-dpe** with an equimolar amount of **bipy**, in the presence of a small amount of MeOH ($\eta = 0.3$).

The expected product was **CP1-bipy**. After 60 minutes of grinding, the solid was washed with MeOH to remove the **dpe** eventually formed. The PXRD trace of the ground material corresponded exactly to that of **CP1-bipy**. Notably, the PXRD analysis conducted on the crude product showed the peaks corresponding to **CP1-bipy** and free **dpe**, indicating that the washing step does not have any influence on the reaction outcome (Fig. S7). Corroborated by the successful preservation of the SBU, we extended the same procedure to the other two

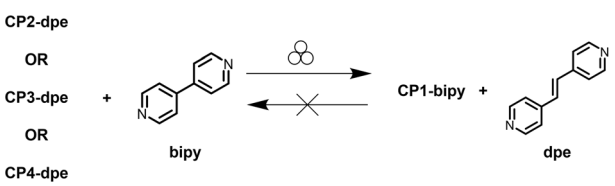

Scheme 2 Mechanochemical post-synthetic modifications (MPSMs) highlighting the irreversible conversion of **dpe**-containing 1D-CPs to **CP1-bipy**.

CPs **CP3-dpe** and **CP4-dpe**. Unexpectedly, in both cases the conversion to **CP1-bipy** was again observed, although with **CP3-dpe** some traces of **CP2-dpe** were detected. In this case, the complete conversion into **CP1-bipy** could be achieved using a two-fold excess of **bipy**. The results indicate that the linker exchange reactions do not occur by a simple linker replacement, but by a substantial structural modification of the SBU, which must occur by partial acetate detachment caused by the replacement of the linker in the coordination sphere of the metal. This can be understood on the basis of the coordinative lability of the acetate group, well proved by its known coordination isomerism. The recurrent formation of **CP1-bipy** confirms, once again, the stability of the ladder structure under mechanochemical conditions when **bipy** is involved. The inverse reaction, corresponding to **bipy** replacement by **dpe** in **CP1-bipy**, was also tested. **CP1-bipy** was then ground in the presence of an equimolar amount of **dpe** using MeOH or water as LAG agents. In both cases, the PXRD analysis of the products evidenced the failure of the reactions (Scheme 2), with the peaks characteristic of the starting materials still clearly visible, pointing out the high stability of the polymer framework of **CP1-bipy**.

Rationalization of the MPSMs of 1D-CPs

While we do not possess a singular explanation of the MPSMs observed in this work, calculations can help to partially rationalize the behavior observed experimentally on the basis of thermodynamic considerations. As depicted in Fig. 5B, **CP1-bipy** is more stable than **CP2-dpe** and **CP3-dpe**. Hence, provided that no new unreported crystalline phases are accessible, the reactions of **CP2-dpe** and **CP3-dpe** with bipy are expected to bring to the formation of **CP1-bipy**, as experimentally confirmed. Moreover, the energy difference between **CP1-bipy** and **CP4-dpe** is negligible, suggesting that the conversion of **CP4-dpe** to **CP1-bipy** is still obtainable, especially if aided by additional factors such as the presence of MeOH as a LAG agent, which was not considered in periodic calculations. Factors such as the inertness of **CP1-bipy** or its relative solubility in MeOH compared to **CP4-dpe** might be invoked but were not experimentally tested. Lastly, it must be stressed that calculations on **CP4-dpe** were necessarily performed in the $P2_1/c$ space group to remove the disorder of the **dpe** ligand (the original space group is $C2/c$) and the presence of a plethora of different ligand arrangements might slightly impact the final stability of the computed structure.

Dimensionality growth: from 1D-CPs to PL-MOFs

The synthetic step responsible for the framework dimensionality growth is based on the replacement of the acetate anion by bridging terephthalate anions (Fig. 1). This means that the intervention of **H_2ta** on the chosen 1D-CP is expected to lead to the elimination of acetic acid. Among the known ML-MOFs containing **dpe**, $[Zn_2(\mathbf{ta})_2(\mathbf{dpe})_2]_n$ (CSD Refcode: SUJQUK)[59] (Fig. 3) can be considered as derived from the simple substitution of the κ^2-chelating acetate ions in **PC2-dpe** with κ^1-monodentate bridging terephthalate dianions, each connecting two adjacent SBUs in the square planes. Hence, we first reacted **PC2-dpe** with an equimolar amount of **H_2ta** (Zn : **H_2ta** molar ratio = 1 : 1) in the presence of a small aliquot of DMF ($\eta = 0.5$), the same solvent used for the solution synthesis of the MOF. The reaction led, after 60 minutes of grinding, to the smooth formation of the expected compound, as can be inferred from the comparison of the experimental and calculated PXRD patterns in Fig. 6 (top and Fig. S8).

Interested to see if it was possible to transfer a geometrically different SBU from a 1D-CP to a PL-MOF, the same reaction was repeated with **CP3-dpe**. Once again, the formation of SUJQUK was observed (Fig. 6, top and Fig. S9), indicating that the simple transfer of the intact tetrahedral SBU in the new framework was unsuccessful. We then focused our attention on **CP4-dpe**, which, upon simple replacement of the bridging acetate ions of the paddle-wheel with **ta^{2-}** anions, would, in principle, yield the known PL-MOF $[Zn_2(\mathbf{ta})_2(\mathbf{dpe})]_n$ (CSD Refcode: AWUVIZ, Fig. 3, right). In this case, the reaction was performed using a Zn : **H_2ta** molar ratio of 1 : 2 to ensure the complete substitution of the acetate anions. The reaction gave a mixture of SUJQUK and

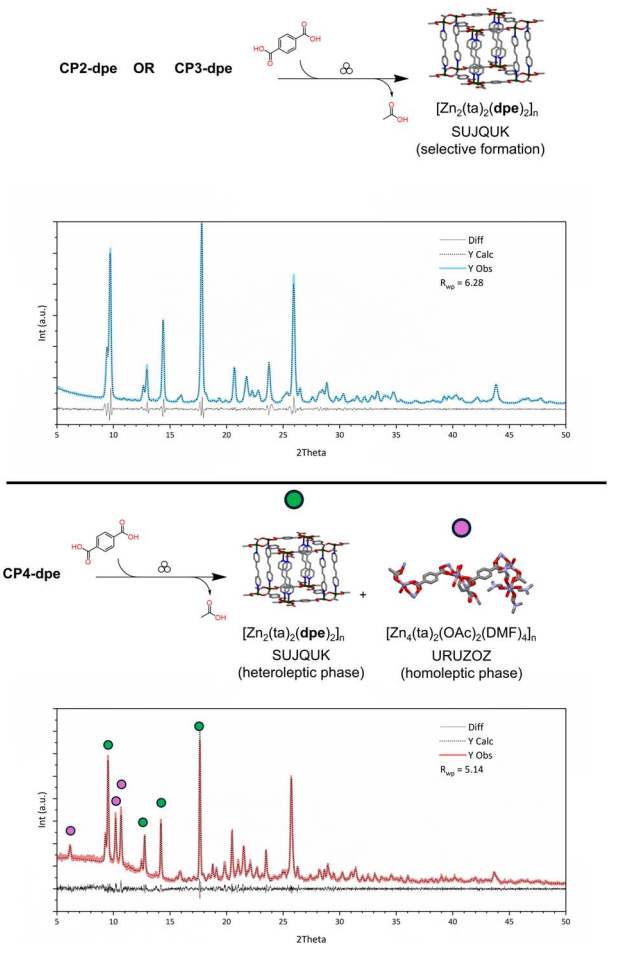

Fig. 6 Dimensionality growth from CP*n*-dpe (n = 2–4) to PL-MOF SUJQUK. Top: reactions involving **CP2-dpe** and **CP3-dpe** leading to the selective formation of SUJQUK (PXRD traces in Fig. S12). Bottom: reaction involving **CP4-dpe** leading to a mixture of SUJQUK and URUZOZ; (PXRD traces in Fig. S13).

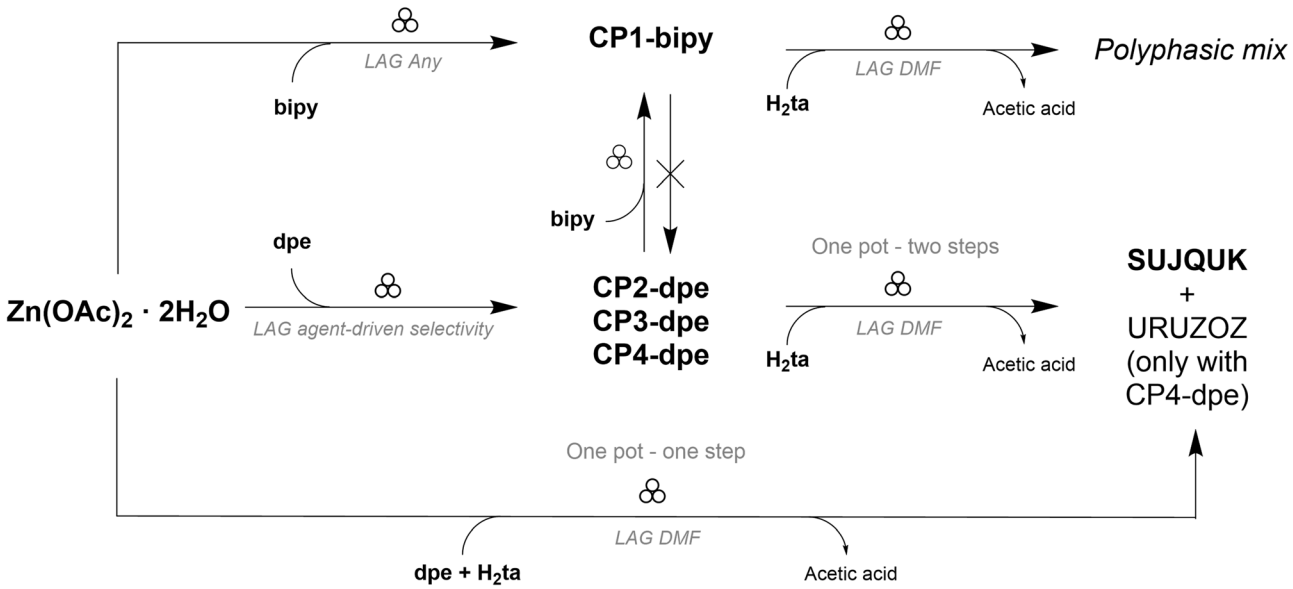

Scheme 3 Complete reaction pathway scheme showing the syntheses of the 1D-CPs, their post-synthetic modifications and the dimensionality growth leading to the PL-MOF SUJQUK.

a second phase lacking **dpe**, with formula $[Zn_4(ta)_3(OAc)_2(DMF)_4]_n$ (CSD Refcode: URUZOZ, Fig. S10).[74] No trace of free **dpe** was visible in the powder diffractogram (Fig. 6, bottom). It is worth noting that the homoleptic polymer was first isolated under solvothermal conditions using a 3D-printed polypropylene autoclave, employing a reactant solution intended to yield the iconic MOF-5 of formula $[Zn_4O(ta)_3]$.[75,76] In that case, its formation was attributed to a partial degradation of the plastic autoclave. In our case, its formation is likely attributable to a mismatched reaction stoichiometry. **CP4-dpe** and SUJQUK present a Zn : **dpe** ratio of 2 : 1 and 1 : 1, respectively. Hence, in the mechanochemical reaction, the amount of ligand **dpe** was insufficient to achieve the right stoichiometry. In fact, the same reaction involving polymers featured by a Zn : **dpe** ratio of 1 : 1, such as **PC2-dpe** and **PC3-dpe**, led to the complete formation of SUJQUK.

Finally, the feasibility to synthesize *via* a one-step procedure, following the reaction pathway c depicted in Fig. 1, was tested. Grinding equimolar amounts of $Zn(OAc)_2 \cdot 2H_2O$, **dpe** and **H_2ta** in the presence of DMF as the LAG agent led to the smooth formation of SUJQUK within 60 minutes of grinding, as can be inferred from Fig. 5 (Fig. S11). Notably, repeating the same reaction with a Zn : **dpe** : **H_2ta** ratio of 2 : 1 : 2 resulted in a mixture of SUJQUK and URUZOZ, as expected. This outcome confirms that the formation of URUZOZ occurs under conditions where **dpe** is deficient in the jar. Rather unexpectedly, the mechanochemical reaction between **PC1-bipy** and **H_2ta**, carried out using DMF as the LAG agent, did not yield a single, well-defined product. Despite multiple attempts to optimize the reaction conditions—including variations in stoichiometric ratios, choice and volume of the LAG solvent, and milling time (tested up to 90 minutes)—the outcome consistently resulted in a complex mixture of unidentified phases. A one-step reaction involving $Zn(OAc)_2 \cdot 2H_2O$, **H_2ta** and **bipy** was also tested, resulting in the same mixtures of unidentified products. A complete overview of the mechanochemical transformations described in this work is depicted Scheme 3.

Green metrics

To evaluate the environmental benefit coming from mechanochemistry, the environmental factor (EF) and reaction mass efficiency (RME) of selected mechanochemical reactions were calculated and compared with those of the corresponding solution-based syntheses. The latter were inferred from the experimental details reported in the respective cited references. As representative reactions, we selected the synthesis of **CP1-bipy** and the one-pot procedure for the synthesis of SUJQUK. Further details of the performed calculations can be found in the SI. Notably, for the synthesis of **CP1-bipy**, a significant reduction of the *E* factor is found, from 114.40 in the wet procedure to ≤0.5 in the mechanochemical one. A similar trend is seen for the synthesis of SUJQUK, where the *E* factor decreases from 121 (solution synthesis) to 1.34 (mechanochemical synthesis). The RME factors also show substantial improvements: from 35.12% to 73.86% for **CP1-bipy** and from 41.61% to 77.71% for SUJQUK, respectively.

Experimental section

General methods

4,4′-Bipyridine (**bipy**), 1,2-bis(4-pyridyl)ethylene (**dpe**), terephthalic acid (**ta**) and $Zn(OAc)_2 \cdot 2H_2O$ were commercially available and used as received. The solvents used for LAG were used without any pre-treatment. The solvents used were methanol (MeOH), dichloromethane (DCM), acetonitrile (ACN), *N*,*N*-dimethylformamide (DMF), tetrahydrofurane (THF) and distilled water (H_2O).

PXRD characterization

PXRD data were collected in Bragg–Brentano geometry with Cu Kα radiation on a Rigaku SmartLab XE diffractometer equipped with a solid-state Hypix3000 2D detector. The samples were placed on glass supports and exposed to radiation ($1.5° \leq 2\theta \leq 50°$) with a scan of $10°\ min^{-1}$. A length-limiting slit of 15 mm was used to exploit the maximum loading of the sample holder; 5° Soller slits were employed to improve the peak profile and limit the overlapping of reflections.

Computational methods

Nonperiodic simulations. DFT calculations were performed at the M06-2x/cc-pvtz level of theory within the framework of the quantum chemistry package Gaussian16.[71] For this analysis, we considered small complexes of zinc(II) metals, pyridine and acetate ligands in the same geometries and stoichiometries as encountered in the experimental crystal structures obtained in this work. Geometries comprised a tetrahedral coordination ("Tet" in Fig. 5), a distorted octahedral, "ladder-like" coordination ("Ld" in Fig. 5), a distorted paddle-wheel ("D-PW" in Fig. 5) and a complete paddle-wheel ("PW" in Fig. 5). "Ld", "D-PW" and "PW" complexes were computed in their dimeric form to allow for an easier comparison with the experimental structures (an accurate depiction of the complexes considered is given in the SI, Fig. S19–S22, the energies are always reported per Zn mole). Relevant thermodynamic parameters were extracted by means of frequency calculation. The calculation is repeated at the same level of theory approximating the effect of three different solvents by means of the SMD method (water, methanol and *N*,*N*′-dimethylformamide). Free energy of reaction was then extracted by subtracting the energy of the reactants to those of the products in the appropriate stoichiometries.

Periodic structure optimization. All calculations were performed within the framework of the program CASTEP23.1.[72] The input models were derived from the experimental single crystal X-ray diffraction structures. The wave function was expanded in plane waves to a kinetic energy cutoff of 1100 eV. The electronic structure was sampled on a *Γ*-centered *k*-point grid with a spacing no greater than $0.07\ Å^{-1}$. For all simulations, the exchange-correlation functional of Perdew–Burke–Ernzerhof (PBE)[77] was used with the dispersion correction of Tkatchenko–Scheffler (TS).[78] The core-valence interaction was modeled with a norm-conversing pseudopotential generated on the fly, as implemented in CASTEP. Convergence was accepted when residual atomic forces reached $<1 \times 10^{-4}$ eV $Å^{-1}$, with SCF convergence accepted at $<1 \times 10^{-10}$ eV. The simulated unit cells agreed well with the experimentally obtained ones (Table S10). The space group of **CP4-dpe** was changed to $P2_1/c$ from $C2/c$ to remove the disorder of the **dpe** ligand (updated atom coordinates are given in the SI, Table S11).

Mechanochemical syntheses

All the reactions were conducted by means of a vibrating ball-mill Retsch MM400 using a 5 mL stainless steel jar equipped with a ball of the same material having a diameter of 7 mm and a weight of 3 g. Where necessary, a small aliquot of solvent was added by means of a micropipette, keeping the ratio μL solvent per mg solids (η value) between 0 and 2 $\mu L\ mg^{-1}$. The jar was shacken at 20 Hz, unless otherwise stated, for the desired time, and the solid withdrawn was vacuum dried and analyzed by FTIR and PXRD analysis. When necessary, the ground solid was subjected to washing with a selected solvent prior to analysis. Structural matching was determined by comparing the experimental PXRD traces with those calculated from the single-crystal structure of the target compound.

Synthesis of the 1D-CPs

*$[Zn_2(OAc)_4(\mu\text{-bipy})_2]_n$ (**CP1-bipy**).* $Zn(OAc)_2 \cdot 2H_2O$ (164.62 mg, 0.75 mmol) and **bipy** (117.13 mg, 0.75 mmol) were used. For the reactions conducted under LAG conditions, the solvents used (100 μL) were MeOH, DCM, ACN, DMF, THF and H_2O. The reaction was conducted at 20 Hz. In all cases, the complete conversion of the reagents into **CP1-bipy** was observed (CSD Refcode: ALUPUS). The reaction conducted under neat conditions contained a higher amount of amorphous phase, as evidenced by PXRD analysis.

FTIR (cm^{-1}): 3075, 3043, 3989, 3924, 1602, 1488, 1418, 1407, 1332, 1238, 1217, 1067, 1044, 1005, 932, 884, 818, 731, 672, 649, 622, 464. Elemental analysis: calcd (%) for $C_{28}H_{28}N_4O_8Zn_2$: C, 49.51; H, 4.15; N, 8.25. Found (%): C, 49.21; H, 4.17; N, 8.01.

*$[Zn_2(OAc)_4(\mu\text{-dpe})_2]_n$ (**CP2-dpe**).* $Zn(OAc)_2 \cdot 2H_2O$ (164.6 mg, 0.75 mmol), **dpe** (136.67 mg, 0.75 mmol) and 100 μL of solvent (MeOH, DMF and THF) were used. The reaction was conducted at 20 Hz. In all cases, the complete conversion of the reagents into **CP2-dpe** was observed (CCDC Refcode: MANMEU).

FTIR (cm^{-1}): 3067, 3012, 1600, 1503, 1419, 1381, 1326, 1250, 1207, 1072, 1014, 988, 832, 666, 650, 617, 552. Elemental analysis: calcd (%) for $C_{32}H_{32}N_4O_8Zn_2$: C, 52.55; H, 4.41; N, 7.66. Found (%): C, 52.59; H, 4.40; N, 7.49.

*$\{[Zn(OAc)_2(\mu\text{-dpe})][H_2O]\}_n$ (**CP3-dpe**).* As for **CP1-dpe** but adding 100 μL of H_2O. The complete conversion of the reagents into **CP3-dpe** was observed (CCDC Refcode: BUJDES).

FTIR (cm^{-1}): 3533, 3012, 2925, 1607, 1581, 1507, 1434, 1391, 1329, 1077, 1027, 986, 927, 832, 670, 619, 550. Elemental analysis: calcd (%) for $C_{16}H_{18}N_2O_5Zn$: C, 50.08; H, 4.73; N, 7.30. Found (%): C, 50.59; H, 4.40; N, 7.49.

*$[Zn_2(OAc)_4(\mu\text{-dpe})]_n$ (**CP4-dpe**).* $Zn(OAc)_2 \cdot 2H_2O$ (219.51 mg, 1 mmol), **dpe** (31.11 mg, 0.5 mmol) and 100 μL of solvent (MeOH, THF and H_2O) were used. The reaction was conducted at 20 Hz. In all cases, the complete conversion of the reagents into **CP4-dpe** was observed (CCDC Refcode: MANLUJ).

FTIR (cm^{-1}): 3063, 3046, 2971, 2924, 1626, 1613, 1509, 1423, 1346, 1296, 1251, 1229, 1080, 1030, 990, 842, 665, 622, 571, 554. Elemental analysis: calcd (%) for $C_{20}H_{22}N_2O_8Zn_2$: C, 43.74; H, 4.04; N, 5.10. Found (%): C, 43.49; H, 4.02; N, 4.91.

General procedure for post-synthetic modifications (MPSMs)

Interconversion reactions of 1D-CPs. The starting polymer (**CP1-bipy** or **CPn-dpe**, n = 2–4) was prepared as previously reported, then an amount of **dpe** or **bipy** corresponding to a Zn : ligand = 1 : 1 molar ratio was added, followed by 100 μL of

solvent (MeOH or H_2O). The jar was closed and shaken at 20 Hz for 60 minutes. The resulting solid was removed from the jar, washed with MeOH to remove the undesired side products, vacuum dried and analyzed by PXRD analysis.

Synthesis of PL-MOFs (CSD Refcode: SUJKUK). Dimensionality growth: the 1D-CP (CP*n*-dpe, $n = 2$, 4) and the desired amount of **H_2ta** were introduced in the jar, followed by 200 μL of DMF as the LAG agent. The jar was closed and shaken for 60 minutes. The resulting solid was removed from the jar, eventually washed with DMF, vacuum dried and analyzed by PXRD analysis.

Reaction involving **CP2-dpe**: **H_2ta** (83.07 mg, 0.50 mmol), **CP2-dpe** (183.86 mg, 0.25 mmol), complete conversion of the reagents to give a mixture of SUJKUK and URUZOZ.

Reaction involving **CP3-dpe**: **H_2ta** (49.84 mg, 0.30 mmol), **CP3-dpe** (110.31, 0.30 mmol), complete conversion to SUJKUK.

Reaction involving **CP4-dpe**: **H_2ta** (83.07 mg, 0.50 mmol), **CP4-dpe** (122.27, 0.25 mmol), complete conversion to SUJKUK.

Direct synthesis. $Zn(OAc)_2 \cdot 2H_2O$ (109.75 mg, 0.5 mmol), **H_2ta** (83.07 mg, 0.5 mmol) and **dpe** (91.11 mg, 0.5 mmol) were introduced in the jar together with 200 μL of DMF. The jar was shaken for 60 minutes. The product was removed from the jar, eventually washed with DMF, vacuum dried and analyzed by PXRD analysis. Complete conversion into SUJKUK was observed.

All the attempts aimed at converting **PC1-bipy** into a PL-MOF failed, leading to a complex polyphasic mixture.

Conclusions

In this work, we successfully employed mechanochemistry for the selective synthesis of various one-dimensional coordination polymers derived from the combination of two pyridyl-containing linkers (**bipy** and **dpe**) with $Zn(OAc)_2 \cdot 2H_2O$. By carefully selecting the reagent ratios and the type of solvent used as a LAG agent, we selectively obtained different crystalline frameworks containing different secondary building units (SBUs), reproducing products previously synthesized by solution-based methods, but with higher yields and significantly greener protocols. Post-synthetic modifications *via* linker exchange reactions were also carried out under mechanochemical conditions, demonstrating the facile and complete transformation of **dpe**-based polymers into a **bipy**-based polymer. A computational approach provided insights into the observed selectivity by comparing the relative stability of the involved SBUs and frameworks. Finally, the efficient synthesis of a three-dimensional pillared metal–organic framework was accomplished through two alternative and convergent strategies: (i) a stepwise approach involving the dimensional expansion of **dpe**-containing 1D polymers *via* grinding with terephthalic acid in the presence of DMF as a LAG agent; and (ii) a one-pot synthesis where all components were simultaneously ground under similar conditions. The set of mechanochemical reactions described is reported in Scheme 3. This work highlights not only the effectiveness of mechanochemistry as a green tool for the selective construction of coordination polymers, but also its efficacy in well controlled post-synthetic modifications and in promoting framework dimensionality growth. Considering the important role that coordination polymers, particularly MOFs, are expected to play in the future, the development of green end efficient protocols for their shaping is of real importance.

Author contributions

The manuscript was written through contributions of all authors. All authors have given approval to the final version of the manuscript.

Conflicts of interest

There are no conflicts to declare.

Data availability

The data supporting this article have been included as part of the supplementary information (SI). Supplementary information: PXRD traces, FTIR spectra, green metrics calculation, and computational details. See DOI: https://doi.org/10.1039/d5mr00106d.

Acknowledgements

The authors thank the Laboratorio di Strutturistica Chimica M. Nardelli of the University of Parma for X-ray data collections. GC acknowledges the Italian Ministry of University and Research (MUR) for funding the PhD scholarship in Chemical Sciences under DM 118/2023. This work has benefited from the equipment and framework of the COMP-R (2023–2027) Initiatives, funded by the Italian Ministry for Education, University and Research program for the "Departments of Excellence". This work also benefited from the 2020 and 2022 calls of the PRIN: Research Projects of Relevant Interest program of the Italian Ministry for University and Research PRIN 2020Y2CZJ2 (NICE-Natural Inspired Crystal Engineering) and PRIN 202224KAX8 (FLIPPER: FLuorinated PePtidEs for Resumption).

Notes and references

1 T. Friščić, C. Mottillo and H. M. Titi, Mechanochemistry for Synthesis, *Angew. Chem., Int. Ed.*, 2020, **59**, 1018–1029.
2 J. L. Howard, Q. Cao and D. L. Browne, Mechanochemistry as an emerging tool for molecular synthesis: what can it offer?, *Chem. Sci.*, 2018, **9**, 3080–3094.
3 J. Batteas, K. G. Blank, E. Colacino, F. Emmerling, T. Friščić, J. Mack, J. Moore, M. E. Rivas and W. Tysoe, *RSC Mechanochem.*, 2025, **2**, 10–19.
4 D. V. N. Prasad and J. Theuerkauf, Effect of grinding media size and chamber length on grinding in a spex mixer mill, *Chem. Eng. Technol.*, 2009, **32**, 1102–1106.
5 P. Sharma, C. Vetter, E. Ponnusamy and E. Colacino, Assessing the Greenness of Mechanochemical Processes with the DOZN 2.0 Tool, *ACS Sustainable Chem. Eng.*, 2022, **10**, 5110–5116.

6 K. J. Ardila-Fierro and J. G. Hernández, Sustainability Assessment of Mechanochemistry by Using the Twelve Principles of Green Chemistry, *ChemSusChem*, 2021, **14**, 2145–2162.
7 F. Cuccu, L. De Luca, F. Delogu, E. Colacino, N. Solin, R. Mocci and A. Porcheddu, Mechanochemistry: New Tools to Navigate the Uncharted Territory of "Impossible" Reactions, *ChemSusChem*, 2022, **15**, e202200362.
8 A. A. L. Michalchuk, M. Trestman, S. Rudic, P. Portius, P. T. Fincham, C. R. Pulham and C. A. Morrison, Predicting the reactivity of energetic materials: an: ab initio multi-phonon approach, *J. Mater. Chem. A*, 2019, **7**, 19539–19553.
9 M. Senna and A. A. L. Michalchuk, *RSC Mechanochem.*, 2025, **2**, 351–369.
10 G. Rothenberg, A. P. Downie, C. L. Raston and J. L. Scott, *J. Am. Chem. Soc.*, 2001, **123**, 8701–8708.
11 R. Freund, et al., The Current Status of MOF and COF Applications, *Angew. Chem., Int. Ed.*, 2021, **60**, 23975–24001.
12 A. Kirchon, L. Feng, H. F. Drake, E. A. Joseph and H. C. Zhou, From fundamentals to applications: a toolbox for robust and multifunctional MOF materials, *Chem. Soc. Rev.*, 2018, **47**, 8611–8638.
13 L. Gagliardi and O. M. Yaghi, Three Future Directions for Metal-Organic Frameworks, *Chem. Mater.*, 2023, **35**, 5711–5712.
14 T. Ghanbari, F. Abnisa and W. M. A. Wan Daud, A review on production of metal organic frameworks (MOF) for CO_2 adsorption, *Sci. Total Environ.*, 2020, **707**, 135090.
15 Z. Ji, H. Wang, S. Canossa, S. Wuttke and O. M. Yaghi, Pore Chemistry of Metal–Organic Frameworks, *Adv. Funct. Mater.*, 2020, **30**, 2000238.
16 J. Wang, et al., A comprehensive transformer-based approach for high-accuracy gas adsorption predictions in metal-organic frameworks, *Nat. Commun.*, 2024, **15**, 1–14.
17 R. Oktavian, et al., Gas adsorption and framework flexibility of CALF-20 explored via experiments and simulations, *Nat. Commun.*, 2024, **15**, 1–10.
18 F. Afshariazar and A. Morsali, The unique opportunities of mechanosynthesis in green and scalable fabrication of metal-organic frameworks, *J. Mater. Chem. A*, 2022, **10**, 15332–15369.
19 S. Głowniak, B. Szczęśniak, J. Choma and M. Jaroniec, Mechanochemistry: toward green synthesis of metal–organic frameworks, *Mater. Today*, 2021, **46**, 109–124.
20 Y. Li, et al., Synthesis and shaping of metal-organic frameworks: a review, *Chem. Commun.*, 2022, **58**, 11488–11506.
21 I. Senkovska, V. Bon, L. Abylgazina, M. Mendt, J. Berger, G. Kieslich, P. Petkov, J. L. Fiorio, J.-O. Joswig, T. Heine, L. Schaper, C. Bachetzky, R. Schmid, R. A. Fischer, A. Poppl, E. Brunner and S. Kaskel, Understanding MOF Flexibility: An Analysis Focused on Pillared Layer MOFs as a Model System, *Angew. Chem., Int. Ed.*, 2023, **62**, e202218076.
22 S. Pullen and G. H. Clever, Mixed-Ligand Metal-Organic Frameworks and Heteroleptic Coordination Cages as Multifunctional Scaffolds - A Comparison, *Acc. Chem. Res.*, 2018, **51**, 3052–3064.
23 D. Balestri, P. P. Mazzeo, C. Carraro, N. Demitri, P. Pelagatti and A. Bacchi, Stepwise Evolution of Molecular Nanoaggregates Inside the Pores of a Highly Flexible Metal–Organic Framework, *Angew. Chem., Int. Ed.*, 2019, **58**, 17342–17350.
24 D. Balestri, P. P. Mazzeo, R. Perrone, F. Fornari, F. Bianchi, M. Careri, A. Bacchi and P. Pelagatti, Deciphering the Supramolecular Organization of Multiple Guests Inside a Microporous MOF to Understand their Release Profile, *Angew. Chem., Int. Ed.*, 2021, 10194–10202.
25 D. Giovanardi, P. P. Mazzeo, P. Pelagatti and A. Bacchi, Guest Molecules Play Tug of War in a Breathing MOF: The Stepwise Monitoring of an Elastic Framework Deformation via SC-SC Transformations, *Cryst. Growth Des.*, 2023, **23**, 8726–8734.
26 L. Liu, Z. Li, B. Wang, L. Wang, X. Meng and Z. He, Polymeric frameworks constructed from bulky carboxylates and 4,4′-bipyridine linkages: synthesis, crystal structures, and properties, *Cryst. Growth Des.*, 2009, **9**, 5244–5258.
27 M. Du, C. P. Li, C. S. Liu and S. M. Fang, Design and construction of coordination polymers with mixed-ligand synthetic strategy, *Coord. Chem. Rev.*, 2013, **257**, 1282–1305.
28 M. L. Mortensen, J. N. Vo, M. U. Hyder, A. Shrivasta, G. T. McCandless and K. J. Balkus Jr, Transformation of a copper complex to a 1-D coordination polymer to 3-D metal-organic frameworks, *Polyhedron*, 2023, **242**, 116512.
29 B. J. Burnett and W. Choe, Stepwise pillar insertion into metal-organic frameworks: a sequential self-assembly approach, *CrystEngComm*, 2012, **14**, 6129–6131.
30 K. Otsubo, T. Haraguchi, O. Sakata, A. Fujiwara and H. Kitagawa, Step-by-step fabrication of a highly oriented crystalline three-dimensional pillared-layer-type metal-organic framework thin film confirmed by synchrotron X-ray diffraction, *J. Am. Chem. Soc.*, 2012, **134**, 9605–9608.
31 B. J. Burnett, P. M. Barron, C. Hu and W. Choe, Stepwise synthesis of metal - organic frameworks: replacement of structural organic linkers, *J. Am. Chem. Soc.*, 2011, **133**, 9984–9987.
32 R. Haldar and C. Wöll, Hierarchical assemblies of molecular frameworks—MOF-on-MOF epitaxial heterostructures, *Nano Res.*, 2021, **14**, 355–368.
33 Y. Chen, H. Wu, Y. Youan, D. Lv, Z. Qiao, D. An, X. Wu, H. Liang, Z. Li and Q. Xia, Highly rapid mechanochemical synthesis of a pillar-layer metal-organic framework for efficient CH_4/N_2 separation, *Chem. Eng. J.*, 2020, **385**, 123836.
34 T. Friscić and L. Fábián, Mechanochemical conversion of a metal oxide into coordination polymers and porous frameworks using liquid-assisted grinding (LAG), *CrystEngComm*, 2009, **11**, 743–745.
35 B. Parmar, Y. Rachuri, K. K. Bisht and E. Suresh, Syntheses and Structural Analyses of New 3D Isostructural Zn(II) and Cd(II) Luminescent MOFs and Their Application towards Detection of Nitroaromatics in Aqueous Media, *ChemistrySelect*, 2016, **1**, 6308–6315.
36 T. Gao, H.-J. Tang, S.-Y. Zhang, J.-W. Cao, Y.-N. Wu, J. Chen, Y. Wang and K.-J. Chen, Mechanochemical synthesis of

three-component metal-organic frameworks for large scale production, *J. Solid State Chem.*, 2021, **303**, 122547.
37 M. Rautenberg, B. Bhattacharya, C. Das and F. Emmerling, Mechanochemical Synthesis of Phosphonate-Based Proton Conducting Metal-Organic Frameworks, *Inorg. Chem.*, 2022, **61**, 10801–10809.
38 M. Rautenberg, B. Bhattacharya, J. Witt, M. Jain and F. Emmerling, In situ time-resolved monitoring of mixed-ligand metal-organic framework mechanosynthesis, *CrystEngComm*, 2022, **24**, 6747–6750.
39 W. Yuan, T. Friščić, D. Apperley and S. L. James, High Reactivity of Metal–Organic Frameworks under Grinding Conditions: Parallels with Organic Molecular Materials, *Angew. Chem., Int. Ed.*, 2010, **49**, 3916–3919.
40 Z. Jiang, W. Xue, H. Huang, H. Zhu, Y. Sun and C. Zhong, Mechanochemistry-assisted linker exchange of metal-organic framework for efficient kinetic separation of propene and propane, *Chem. Eng. J.*, 2023, **454**(1), 140093.
41 M. Carcelli, A. Bacchi, P. Pelagatti, G. Rispoli, D. Rogolino, T. W. Sanchez, M. Sechi and N. Nemati, Ruthenium arene complexes as HIV-1 integrase strand transfer inhibitors, *J. Inorg. Biochem.*, 2013, **118**, 74–82.
42 P. P. Mazzeo, M. Prencipe, T. Feiler, F. Emmerling and A. Bacchi, On the Mechanism of Cocrystal Mechanochemical Reaction via Low Melting Eutectic: A Time-Resolved in Situ Monitoring Investigation, *Cryst. Growth Des.*, 2022, **22**, 4260–4267.
43 F. Fornari, N. Riboni, C. Spadini, C. S. Cabassi, M. Iannarelli, C. Carraro, P. P. Mazzeo, A. Bacchi, S. Orlandini, S. Furlanetto and M. Careri, Development of novel cocrystal-based active food packaging by a Quality by Design approach, *Food Chem.*, 2021, **347**, 129051.
44 F. Montisci, P. P. Mazzeo, C. Carraro, M. Prencipe, P. Pelagatti, F. Fornari, F. Bianchi, M. Careri and A. Bacchi, Dispensing Essential Oil Components through Cocrystallization: Sustainable and Smart Materials for Food Preservation and Agricultural Applications, *ACS Sustainable Chem. Eng.*, 2022, **10**, 8388–8399.
45 P. P. Mazzeo, S. Canossa, C. Carraro, P. Pelagatti and A. Bacchi, Systematic coformer contribution to cocrystal stabilization: energy and packing trends, *CrystEngComm*, 2020, **42**, 7341–7349.
46 V. Sinisi, P. Pelagatti, M. Carcelli, A. Migliori, L. Mantovani, L. Righi, G. Leonardi, S. Pietarinen, C. Hubsch and D. Rogolino, A Green Approach to Copper-Containing Pesticides: Antimicrobial and Antifungal Activity of Brochantite Supported on Lignin for the Development of Biobased Plant Protection Products, *ACS Sustainable Chem. Eng.*, 2019, **7**(3), 3213–3221.
47 C. Gazzurelli, A. Migliori, P. P. Mazzeo, M. Carcelli, S. Pietarinen, G. Leonardi, A. Pandolfi, D. Rogolino and P. Pelagatti, Making Agriculture More Sustainable: An Environmentally Friendly Approach to the Synthesis of Lignin@Cu Pesticides, *ACS Sustainable Chem. Eng.*, 2020, **8**, 14886–14895.
48 C. Gazzurelli, M. Carcelli, P. P. Mazzeo, C. Mucchino, A. Pandolfi, A. Migliori, S. Pietarinen, G. Leonardi, D. Rogolino and P. Pelagatti, Exploiting the Reducing Properties of Lignin for the Development of an Effective Lignin@Cu_2O Pesticide, *Adv. Sustainable Syst.*, 2022, **6**(8), 2200108.
49 G. Cagossi, P. P. Mazzeo and P. Pelagatti, Mechanochemistry comparison between mechanochemical and solution synthesis of Zn and Cu complexes containing pyridine and p-halogen substituted, *RSC Mechanochem.*, 2025, **2**, 475–481.
50 C. Gazzurelli, M. Solzi, F. Cugini, P. P. Mazzeo, A. Bacchi and P. Pelagatti, Comparison of different synthetic approaches for the fabrication of a bio-inspired 1D-coordination polymer: from solution chemistry to mechanochemistry, *Inorg. Chim. Acta*, 2022, **539**, 121010.
51 B. Conerney, P. Jensen, P. E. Kruger, B. Moubaraki and K. S. Murray, Synthesis and structural characterisation of two coordination polymers (molecular ladders) incorporating $[M(OAc)_2]_2$ secondary building units and 4,4′-bipyridine [M = Cu(II), Zn(II)], *CrystEngComm*, 2003, **5**, 454–458.
52 J. Kim, U. Lee and K. K. Bon, One-dimensional network of zinc(II) coordination polymer with 4,4′-bipyridine (4,4′-bipy), *Bull. Korean Chem. Soc.*, 2006, **27**, 918–920.
53 T. W. Lee, J. P. K. Lau and W. T. Wong, Synthesis and characterization of coordination polymers of Zn(II) with 1,3-bis(4-pyridyl)propane and 4,4′-pyridine ligands, *Polyhedron*, 2004, **23**, 999–1002.
54 L. T. Ni, M. Nagarathinam and J. J. Vittal, Topochemical photodimerization in the coordination polymer $[\{(CF_3CO_2)(\mu\text{-}O_2CCH_3)Zn\}_2(\mu\text{-bpe})_2]_n$ through single-crystal to single-crystal transformation, *Angew. Chem., Int. Ed.*, 2005, **44**, 2237–2241.
55 P. Phuengphai, S. Youngme, N. Chaichit and J. Reedijk, New 3D supramolecular networks built from 1D and 2D frameworks via π-π and H-bonding interactions: topology and catalytic properties, *Inorg. Chim. Acta*, 2013, **403**, 35–42.
56 B. Chen, C. Liang, J. Yang, D. S. Contreras, Y. L. Clancy, E. B. Lobkovsky, O. M. Yaghi and S. Dai, A microporous metal-organic framework for gas-chromatographic separation of alkanes, *Angew. Chem., Int. Ed.*, 2006, **45**, 1390–1393.
57 J. Tao, M. L. Tong and X. M. Chen, Hydrothermal synthesis and crystal structures of three-dimensional co-ordination frameworks constructed with mixed terephthalate (tp) and 4,4′-bipyridine (4,4′-bipy) ligands: [M(tp)(4,4′-bipy)] (M = CoII, CdII or ZnII), *J. Chem. Soc., Dalton Trans.*, 2000, 3669–3674, DOI: 10.1039/b005438k.
58 B. Liu, H.-F. Zhou, Z.-H. Guan, L. Hou, B. Cui and Y.-Y. Wang, Cleavage of a C-C σ bond between two phenyl groups under mild conditions during the construction of Zn(II) organic frameworks, *Green Chem.*, 2016, **18**, 5418–5422.
59 M. H. Mir, L. L. Koh, G. K. Tan and J. J. Vittal, Single-crystal to single-crystal photochemical structural transformations of interpenetrated 3D coordination polymers by [2+2] cycloaddition reactions, *Angew. Chem., Int. Ed.*, 2010, **49**, 390–393.

60 D. Liu, H. X. Li, Y. Chen, Y. Zhang and J. P. Lang, Hydrothermal synthesis and structural characterization of two zinc coordination polymers of 1,2-di(4-pyridyl)ethylene and benzenedicarboxylate, *Chin. J. Chem.*, 2008, **26**, 2173–2178.

61 A. C. Tella, G. Mehlana, L. O. Alimi and S. A. Bourne, Solvent-Free Synthesis, Characterization and Solvent-Vapor Interaction of Zinc(II) and Copper(II) Coordination Polymers Containing Nitrogen-Donor Ligands, *Zeitschrift fur Anorganische und Allgemeine Chemie*, 2017, **643**, 523–530.

62 A. Scano, E. Mereu, V. Cabras, G. Mannias, A. Garau, M. Pilloni, G. Orrù, A. Scano and G. Ennas, Green Preparation of Antimicrobial 1D-Coordination Polymers: $[Zn(4,4'\text{-bipy})Cl_2]_\infty$ and $[Zn(4,4'\text{-bipy})_2(OAc)_2]_\infty$ by Ultrasonication of Zn(II) Salts and 4,4′-Bipyridine, *Molecules*, 2022, **27**(19), 6677.

63 C. J. Adams, H. M. Colquhoun, P. C. Crawford, M. Lusi and A. G. Orpen, Solid-state interconversions of coordination networks and hydrogen-bonded salts, *Angew. Chem., Int. Ed.*, 2007, **46**, 1124–1128.

64 C. J. Adams, M. F. Haddow, M. Lusi and A. G. Orpen, Crystal engineering of lattice metrics of perhalometallate salts and MOFs, *Proc. Natl. Acad. Sci. U. S. A.*, 2010, **107**, 16033–16038.

65 A. Pichon and S. L. James, An array-based study of reactivity under solvent-free mechanochemical conditions - insights and trends, *CrystEngComm*, 2008, **10**, 1839–1847.

66 S. Darwish, S. Q. Wang, D. M. Croker, G. M. Walker and M. J. Zaworotko, Comparison of Mechanochemistry vs Solution Methods for Synthesis of 4,4′-Bipyridine-Based Coordination Polymers, *ACS Sustainable Chem. Eng.*, 2019, **7**, 19505–19512.

67 M. C. Hsu, R. Y. Lin, T. Y. Sun, Y. X. Huang, M.-S. Li, Y.-H. Li, H.-L. Chen and M. Shieh, Inorganic-organic hybrid Cu-dipyridyl semiconducting polymers based on the redox-active cluster $[SFe_3(CO)_9]^{2-}$: filling the gap in iron carbonyl chalcogenide polymers, *Dalton Trans.*, 2024, **53**, 7303–7314.

68 G. C. Laredo, P. M. Vega-Merino, J. A. Montoya-de la Fuente, R. J. Mora-Vallejio, E. Meneses-Ruiz, J. J. Castillo and B. Zapata-Rendon, Comparison of the metal-organic framework MIL-101 (Cr) versus four commercial adsorbents for nitrogen compounds removal in diesel feedstocks, *Fuel*, 2016, **180**, 284–291.

69 M. Y. Masoomi, A. Morsali and P. C. Junk, Rapid mechanochemical synthesis of two new Cd(ii)-based metal-organic frameworks with high removal efficiency of Congo red, *CrystEngComm*, 2015, **17**, 686–692.

70 B. Chen, S. Ma, F. Zapata, F. R. Fronczek, F. B. Lobkovsky and H. C. Zhou, Rationally designed micropores within a metal-organic framework for selective sorption of gas molecules, *Inorg. Chem.*, 2007, **46**(4), 1233–1236.

71 M. J. Frisch, et al., *Gaussian16*, preprint at 2016.

72 S. J. Clark, M. D. Segall, C. J. Pickard, P. J. Hasnip, M. I. J. Probert, K. Refson and M. Payne, First principles methods using CASTEP, *Z. Kristallogr.–Cryst. Mater.*, 2005, **220**(5–6), 567–570.

73 C. Jin, S. Shi, S. Liao, S. Liu, S. Xia, Y. Luo, S. Wang, H. Wang and C. Chen, Post-Synthetic Ligand Exchange by Mechanochemistry: Toward Green, Efficient, and Large-Scale Preparation of Functional Metal-Organic Frameworks, *Chem. Mater.*, 2023, **35**, 4489–4497.

74 G. L. Denisov, P. V. Primakov and Y. V. Nelyubina, A New Metal-Organic Framework: Product of Solvothermal Synthesis in 3D-Printed Autoclaves, *Russ. J. Coord. Chem.*, 2021, **47**, 253–260.

75 M. S. Biserčić, B. Mirjanovic, B. N. Vasiljevic, S. Mentus, B. A. Zasonska and G. Ciric-Marjanovic, The quest for optimal water quantity in the synthesis of metal-organic framework MOF-5, *Microporous Mesoporous Mater.*, 2019, **278**, 23–29.

76 F. Containing and L. Rectangular, Framework containing large rectangular, *J. Am. Chem. Soc.*, 1995, **117**, 10401–10402.

77 J. P. Perdew and M. E. Kieron Burke, Generalized Gradient Approximation Made Simple, *Phys. Rev. Lett.*, 1996, **77**, 3865–3868.

78 A. Tkatchenko and M. Scheffler, Accurate molecular van der Waals interactions from ground-state electron density and free-atom reference data, *Phys. Rev. Lett.*, 2009, **102**, 6–9.